Physica A 179 (1991) 249–268
North-Holland

PHYSICA A

Critical exponents of the sand pile models in two dimensions

S.S. Manna[1]

Höchstleistungsrechenzentrum des Forschungszentrums, Postfach 1913, W-5170 Jülich 1, Germany

Received 2 June 1991

We study three sand pile automaton models namely, the critical height, critical slope and the critical Laplacian models in two dimensions, in which the stability criterion of the sand columns depend on the zeroth, first and the second derivatives of the sand height function. We carried out simulations on system sizes up to 2048×2048 and up to 10^8 avalanches were generated. The exponents of the critical height model were calculated by taking into account the strong corrections to scaling. In order to determine the exponents of the critical Laplacian model accurately we introduced a height restriction in the toppling criterion that maintains universality but accelerates convergence to the steady state by orders of magnitude. We see clear scaling in the critical height and the critical Laplacian models and find that they belong to different universality classes. However, we do not find any scaling in the critical slope model.

1. Introduction

Spatially extended dynamical systems – that is, systems with both temporal and spatial degrees of freedom, evolve into structures with long-range fractal patterns or long-range temporal correlations with $1/f$-type power spectrums. Bak, Tang and Wiesenfeld (BTW) [1] came up with a suggestion that this behaviour may be caused by the self-organization of the systems into a critical state. In this new phenomenon a system under time evolution of its own dynamics creates a critical state where transport takes place perturbing the system repeatedly and the effects of perturbation spread on all length scales and all time scales characterised by the power law distributions. The critical state is independent of the arbitrary initial configuration to start with and unlike ordinary critical phenomena no fine tuning is necessary to arrive at this state. This state is called the self-organized critical state (SOC) and BTW suggested that this process may be the underlying cause of a large class of

[1] Present address: Department of Mathematics, Yale University, New Haven, CT 06520, USA.

phenomena involving dissipative non-linear transport in open systems, such as $1/f$ noise in electrical networks, light pulses from quasers etc. [1]. However, it was demonstrated later that generally the power law scaling distributions do not necessarily lead to non-trivial power laws for the power spectrum different from the trivial $1/f^2$ type variations [2, 3]. Until now experimental work related to SOC have been reported on sand piles [4], water drops on window panes [5] and magnetic domain structures [6]. Recently it has been observed that the local conservation of particle number is not a necessary criterion to achieve the power law distributions [7].

An integer variable h is associated with each site of a square lattice representing the height of the sand column at that site. Starting from an empty lattice one adds sand grains one at a time to a randomly chosen site (i, j) of the lattice

$$h_{i,j} \to h_{i,j} + 1 . \tag{1}$$

The stability of a sand column depends on a preassigned critical condition. In this paper we consider the cases when some derivative of the height function at a certain site is greater than or equal to a preassigned value of the same quantity, the same column becomes unstable and topples. We study three different sand pile models using three different derivatives of the height function. For all models, in a toppling, the height at that site reduces as

$$h_{i,j} \to h_{i,j} - 4 . \tag{2}$$

This amount of sand is distributed equally within the four nearest neighbours, which gain one unit each

$$h_{i\pm1,j\pm1} \to h_{i\pm1,j\pm1} + 1 . \tag{3}$$

Particle number is conserved for topplings within the lattice. For topplings on the boundary sites, however, some grains fall outside the boundary and never come back. After a long time the input (sand addition) and the output (drop through the boundary) rates are equal on the average and the system reaches a critical state. In this state the average sand height fluctuates randomly around a fixed value (depending on the lattice size). For toppling at a site the nearest neighbours gain sand grains. Some of them may be unstable again by violating the stability condition, all of which will topple on the next sweep through the lattice. In this way a cascade of topplings can occur forming an avalanche that ends when no site is unstable.

The cluster size s is defined as the total number of topplings in an avalanche (note that one site may topple more than once in an avalanche).

We define one unit of time consisting of the following four steps.
(a) A list is made of all sites that are unstable.
(b) The heights at all these sites are reduced by four units.
(c) Corresponding to every site of this list one unit is added to each nearest neighbour.
(d) All these sites in the list and their nearest neighbours are searched for unstable sites to make a renewed list.

The life time t of the avalanche is the number of the time units necessary for the avalanche to die.

The size and the life time of the avalanches obey power law distributions [1, 7–11]

$$D'(s) \sim s^{-\tau} , \tag{4}$$

$$D'(t) \sim t^{-y} , \tag{5}$$

and the average life time T_s for cluster size s is scaled as

$$T_s \sim s^{x} . \tag{6}$$

The relation $D(t)\,\mathrm{d}t \sim D(s)\,\mathrm{d}s$ with equations (4)–(6) leads to the scaling relation [2]

$$x = (\tau - 1)/(y - 1) . \tag{7}$$

Zhang has argued that the size distribution exponent τ should be $\tau = 2(1 - 1/d)$ in d dimensions [11, 12]. However, in the models we found scaling, we get $\tau > 1$ in $d = 2$ in contrast to $\tau = 1$ as predicted by Zhang [11, 12].

For the simulation of these three models we used the single cluster growth algorithm to study the avalanche statistics following reference [9]. We measure the probability distributions $D'(s)$ and $D'(t)$ and T_s. To coarse grain the data we integrate these distribution data over exponentially increasing bin lengths of s or t. Therefore we construct the integrated distributions

$$D(s) = \int D'(s)\,\mathrm{d}s \sim s^{1-\tau} \quad \text{and} \quad D(t) = \int D'(t)\,\mathrm{d}t \sim t^{1-y} ,$$

and plot them on the double-logarithmic scales to get the exponents. Estimates of errors in the exponent values have been found by averaging the fluctuations in successive slopes over several bins in all cases.

In the following sections we study sand pile models resulting from a stability condition on the height function itself (section 2), the first derivative of the

height function (section 3) and the second derivative of the height function (section 4). Conclusions are given in section 5.

2. Critical height model (CHM)

In this model the stability of a sand column depends on a preassigned value of the sand height h_c.

The stability condition is that the sand column becomes unstable if $h_{i,j} \geqslant h_c$.

When a sand height topples it loses four particles by eq. (2) and the nearest neighbours gain sand grains of one unit each by eq. (3). In the steady state each site has an equal height on the average, except for the boundaries where the average height is low. This model is a particular case of the general Abelian sand pile model (ASM) [13]. The steady state resulting from the addition of sand grains to the system does not depend on the sequence in which the sand grains are added. This is because in this model the stability of a sand height depends on a critical value of the height itself and the instability of one column does not depend on the toppling of the other sites. The addition of one sand grain to a critical state can be thought of as an operator acting on the critical sate of the sand piles before the addition. These operators follow a commutative operator algebra from which some quantities of the critical height model have been calculated exactly [13].

This model has been studied before [8] and the critical exponents obtained are $\tau = 1.22$ and $y = 1.38$ [8], however, no direct numerical estimate has been given in the literature for the value of the exponent x. The motivation behind the present reanalysis is to get more accurate exponent values so as to make comparisons with other models whose exponents are close. In the present study we could go to the very large lattice sizes up to $L = 2048$ and with very large sample sizes (see table I).

We first present the raw data for the integrated probability distribution $D(s)$ for the square lattice on a double-logarithmic plot with the cluster size s (see

Table I
The number of avalanches (in millions) used for studying different models for different lattice sizes.

Lattice size		16	32	64	128	256	512	1024	2048
CHM	square	32.2	217.9	81.8	50.1	22.3	19.4	3.88	0.10
	triangular	149.8	68.3	14.8	133.2	11.5	9.9	2.16	
CSM	square		48.5	20.9	4.4	1.31			
CLM	square		55.0	7.8	1.8				
Restricted CLM	square					1.6	0.81	0.22	

fig. 1a) for the lattice sizes $L = 16$ to 2048 increases by a factor of two. We see that for different lattice sizes L the curves have some structure and no curve is very straight from very small cluster sizes to the large ones. Even the average slopes for the curves are different and the slope increases as the system size increases. In ref. [8] we extrapolated these slopes with $1/\ln L$ to get the

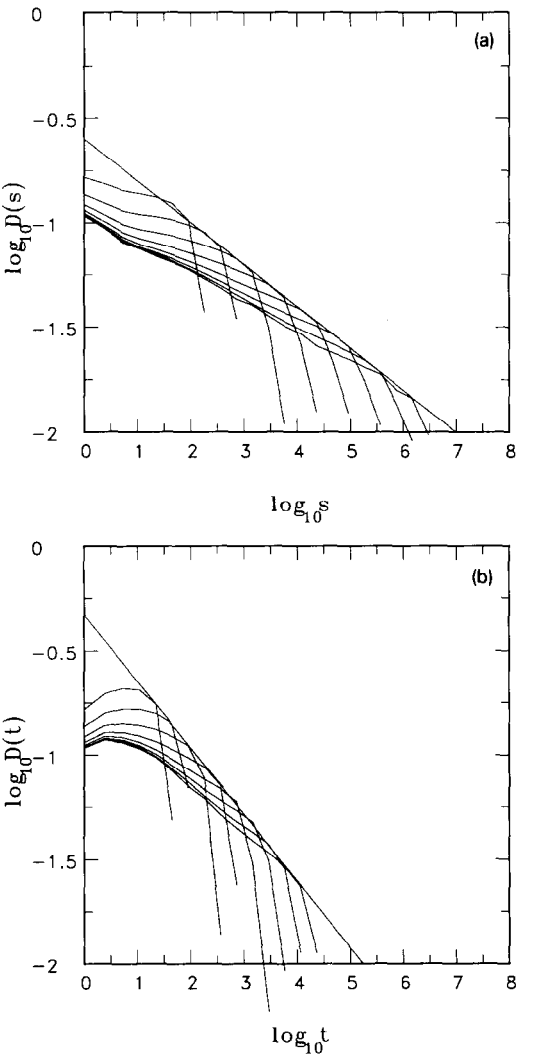

Fig. 1. Cluster distributions for the CHM. (a) The integrated cluster size distribution $D(s)$ plotted against the cluster size s for different lattice sizes ranging from $L = 16$ to 2048 increased by a factor of two (from left to the right). The straight line is the envelope of these curves and has a slope of 0.2007. (b) The integrated life time distribution $D(t)$ plotted against the life time t for the same lattice sizes as in (a) and the envelope has a slope of 0.319. (c) The average life time T_s for an avalanche of size s is plotted against s. The straight line has a slope of 0.607.

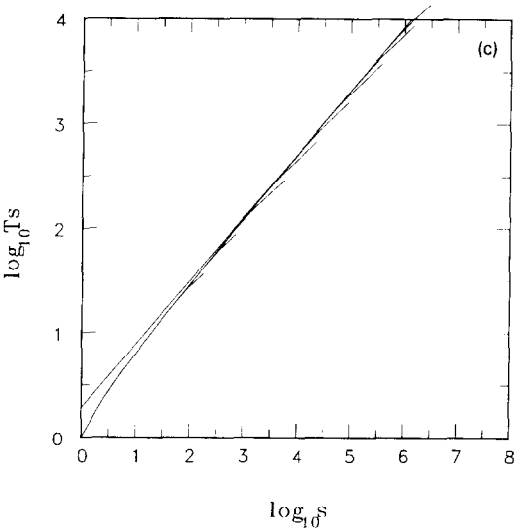

Fig. 1 (cont.).

asymptotic value of $\tau = 1.22$. The left-hand ends of these curves (points for cluster size $s = 1$) approach very quickly to their asymptotic values as $1/L$.

$$D_{s=1}(L) = D_{s=1}(\infty) + A/L \, .$$

Extrapolating $D_{s=1}(L)$ values for different lattice sizes L as $1/L$ we get $D_{s=1}(\infty) = 0.108$ and $A = 0.926$ for the square lattice. For very large cluster sizes the curves bend down showing the finite size of the lattice. However, we observe that all these curves at these points of bending touch a common envelope. We find this envelope is very straight, other than for the system size $L = 16$ all curves touch the same straight line without having any curvature. We also observe that the touching point on this straight line shifts an equal distance as the lattice size is doubled. Therefore we argue that for the infinite system size the curve will start from a point corresponding to $D_{s=1}(\infty)$ and it would touch this straight envelope at infinity, which means the curve for the infinite system size will be parallel to the envelope. Therefore we measure the slope of the envelope accurately, which gives a value for the exponent $\tau = 1.2008$. As the left end of the curve is almost fixed at the point $D_{s=1}(\infty)$ and the touching point with the envelope shifts an equal distance on the envelope we see that the slopes increase as $1/\ln L$. Therefore we conjecture that the exponent τ approaches its asymptotic limit with a dominant $1/\ln L$ correction as

$$\tau(L) = \tau(\infty) - \text{const.}/(\ln L) \, .$$

However when we extrapolate the $\tau(L)$ values from our present data we get $\tau(\infty) = 1.22$, which shows that our large-size simulation is still not sufficient to give an accurate exponent value on extrapolating with this correction.

Similarly we study the life time distribution and plot the integrated life time distribution $D(t)$ with the life time t in a double-logarithmic plot for the same lattice sizes as before (see fig. 1b). Here we also see that all curves touch an envelope before bending down and the envelope is a straight line for large system sizes. We measure the slope of this straight line to get the value of the exponent $y = 1.319$.

Next we study how the average life time T_s scales with the cluster size s. We calculate T_s for each bin length and plot on a double-logarithmic scale (see fig. 1c). We see that curve has considerable initial curvature and the best straight portion starts at very large cluster sizes. We measure the slope at this region to get the exponent $x = 0.607$.

We did a similar calculation for the triangular lattice up to the system size $L = 1024$ and obtain $D_{s=1}(\infty) = 0.1377$, $A = 1.159$ and $\tau = 1.2007$, $y = 1.313$ and $x = 0.609$. We average the values of the three exponents for the square and the triangular lattices and conclude that in two dimensions $\tau = 1.2007 \pm 0.0050$, $y = 1.316 \pm 0.030$, and $x = 0.608 \pm 0.040$. Using the values of τ and y we get from eq. (7) a value for $x = 0.635$ which is 4.5 per cent away from our estimate.

3. Critical slope model (CSM)

In this model a sand column topples when the local slope (first derivative of the height function) in any of the four directions reaches a preassigned value.

The stability condition is if $h_{i,j} - h_{i+1,j} \geq z_c$ or $h_{i,j} - h_{i,j+1} \geq z_c$ or $h_{i,j} - h_{i-1,j} \geq z_c$ or $h_{i,j} - h_{i,j-1} \geq z_c$, then the sand column becomes unstable. This means if at least one slope in any of the four directions reaches the critical slope z_c then the sand column topples.

When a sand column topples it loses four particles by eq. (2) and the nearest neighbours gain one unit each by eq. (3). The boundary external to the lattice is always maintained at zero height. This model has not been studied before.

In this model the steady state resulting from the addition of a number of sand grains to the system depends on the sequence of the sand grains added. This can be understood by considering two sites that are unstable at a certain instant. Toppling one of them will result in sand grain additions to the nearest neighbours and that may destroy the instability of the other unstable site. Therefore the CSM is a non-Abelian sand pile model.

We first see how the average height in the steady state $\langle h \rangle$ varies with the critical value of the local slope z_c. We always start from an empty lattice. For $z_c \leq 3$ we see that after a few avalanches one infinite avalanche starts that never stops and it continuously digs out sand and throws it outside the lattice so that the hole depth continuously increases. However from $z_c = 4$ and onwards we get a stable sand pile with a positive height.

The shape of the sand pile in the CSM is very much like a pyramid. Puhl has also obtained sand piles of pyramidal shape [14]. A typical picture of a sand pile for $z_c = 5$ and $L = 64$ is shown in the fig. 2. The variation of the average height $\langle h \rangle$ with the critical slope z_c is shown in the fig. 3 for $L = 16$, 32 and 64. We see that after some curvature the variation is approximately linear. In general we write a variation of $\langle h \rangle$ with z_c as

$$\langle h \rangle = (0.18L)z_c - 0.39L ,$$

which implies that the average height for a particular value of z_c grows with the system size as $\langle h \rangle \sim L$.

The number of sand grains needed to reach the critical state varies with the system size. Starting from an empty lattice the number of particles n_c needed to

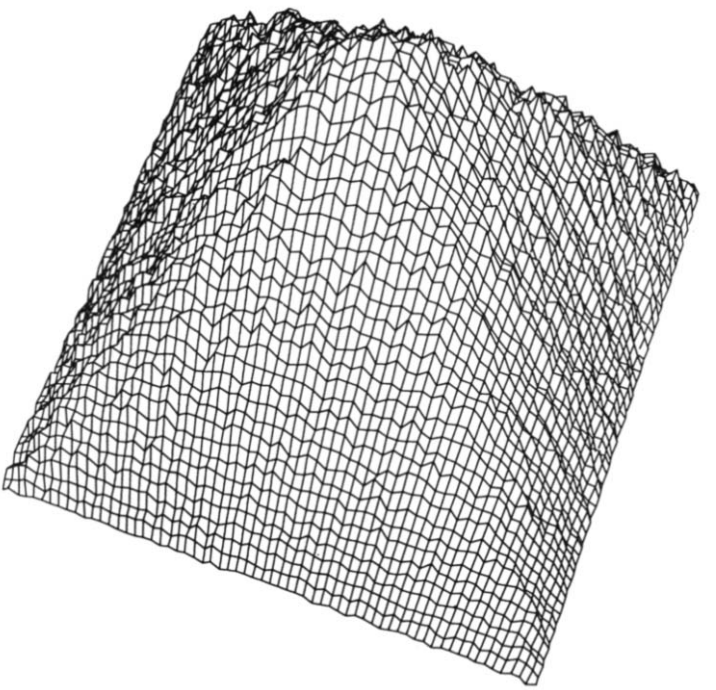

Fig. 2. A typical CSM sand pile on a square lattice of $L = 64$ and for the critical slope $z_c = 5$.

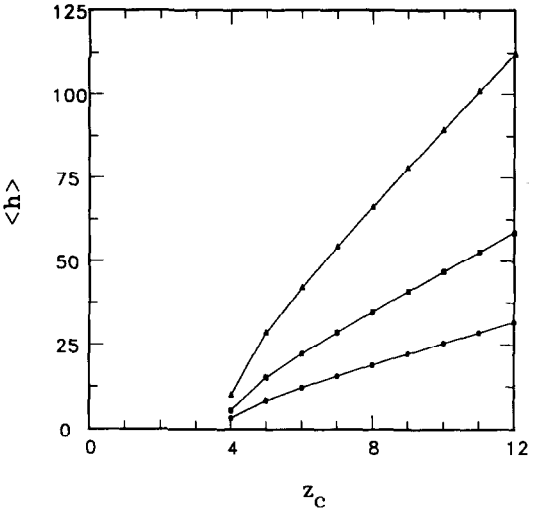

Fig. 3. Variation of the average height $\langle h \rangle$ in the CSM with the critical slope z_c for different lattice sizes $L = 16$ (filled circles), $L = 32$ (boxes) and $L = 64$ (triangles).

add to the system to reach that stage when the average height increases no more varies with the lattice size L approximately as

$$n_c \sim L^3 .$$

Next we study the avalanche cluster statistics. As the number of particles needed to reach criticality increases as L^3 we could simulate only up to $L = 256$. One may argue that we could have started our simulation by dropping sand grains on a regular pyramid of the same size as we obtained in this model and then continue dropping a little at a time to reach the criticality. However we did not use this method because we believe that as the CSM is a non-Abelian model the final critical state may depend on the starting initial configuration. To compare our different models we always started from the initial empty configuration. In fig. 4a we present the double-logarithmic plot of the integrated cluster size distribution $D(s)$ with s for $z_c = 4$ and for $L = 32$, 64, 128 and 256. We have checked that for $z_c = 5$ that the distribution is similar. We see a very large hump in each curve; the hump width and the area under the hump increase as the lattice size is increased. We could not find a straight region in these curves.

We show the life time distribution $D(t)$ plotted against t in the fig. 4b. We see that similar humps are present in these curves. In the fig. 4c we plot the average life time T_s for the cluster size s. We see that the curve has

considerable curvature everywhere and no straight region is found. We conclude that there is no simple scaling in CSM.

Puhl [14] is at present studying a critical slope model in which he uses a quenched randomness for the asymmetric critical slopes z_c and, in a toppling, particles are donated to the nearest neighbours in a random order. This model shows the presence of scaling.

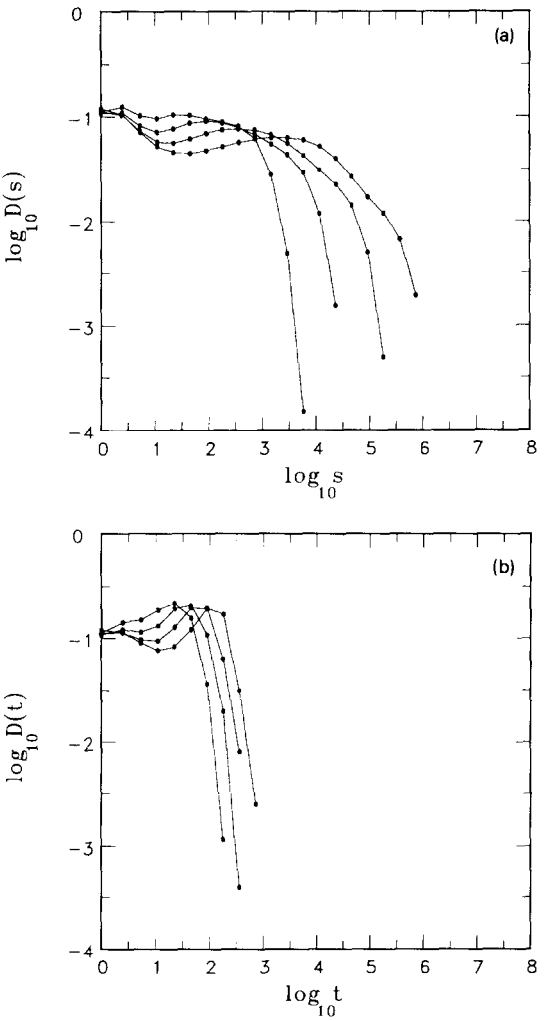

Fig. 4. Cluster distributions for the CSM. (a) The integrated cluster size distribution $D(s)$ is plotted against the cluster size s for lattice sizes $L = 32$, 64, 128 and 256 (from left to the right). (b) The integrated life time $D(t)$ is plotted against the life time t for the same lattice sizes as in (a). (c) The average life time T_s for a cluster s is plotted against the cluster size s.

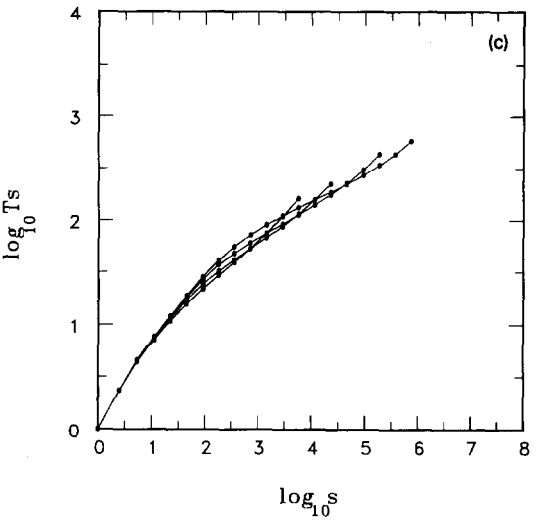

Fig. 4 (cont.).

4. Critical Laplacian model (CLM)

In this model a sand column topples when the local Laplacian (second derivative of the height function) reaches a preassigned value. The local Laplacian $l_{i,j}$ is defined as

$$l_{i,j} = 4h_{i,j} - h_{i+1,j} - h_{i,j+1} - h_{i-1,j} - h_{i,j-1} .$$

The stability condition is: if $l_{i,j} \geq l_c$ then the sand column becomes unstable.

When a sand pile topples it loses four particles by eq. (2) and the nearest neighbours gain one unit each of sand grains by eq. (3). The boundary external to the lattice is always maintained at zero height.

The local Laplacian can be related to the gravitational energy loss in a toppling of a sand column. A sand grain at a height h has potential energy h (with mass of the grain and field strength equal to unity). A sand column of height h has total energy $h(h+1)/2$. In a height toppling four grains from the top fall on the nearest neighbours, losing an energy $4h - 6$ in the process. Every neighbouring site gains one grain and gains energy. Therefore the net loss of energy in one toppling is

$$4h_{i,j} - h_{i+1,j} - h_{i,j+1} - h_{i-1,j} - h_{i,j-1} - 10 .$$

Kadanoff et al. studied the CLM (note that they called this model the

critical-slope model) and from a scaling analysis they claimed this model belongs to a different universality class [10].

In this model the instability of the sand column also depends on the state of the other sand columns. At a certain time an unstable sand column may become stable because of toppling of the other sand columns. Therefore CLM is also a non-Abelian sand pile model.

We first see how the average height in the steady state $\langle h \rangle$ varies with the critical value of the local Laplacian l_c. In fig. 5 we see this variation from $l_c = 1$ to 16 for three lattice sizes $L = 10$, 20 and 40. All these three curves are straight lines and pass through the point $l_c^* = 8.66 \pm 0.10$ on the line $\langle h \rangle = 0$. Below $l_c^* = 8.66$ the average height is negative. We always start from a lattice with zero heights at all sites and the boundary external to the lattice is always maintained at zero height. We see for $l_c \leq 8$ first that a few avalanches are very large and these avalanches dig a hole, throwing all the material outside the lattice and the system reaches a steady state. In general we can write the variation of $\langle h \rangle$ with l_c as

$$\langle h \rangle = (0.038L^2)l_c - 0.33L^2 ,$$

which shows that the average height $\langle h \rangle$ for a particular value of l_c grows with the system size as $\langle h \rangle \sim L^2$.

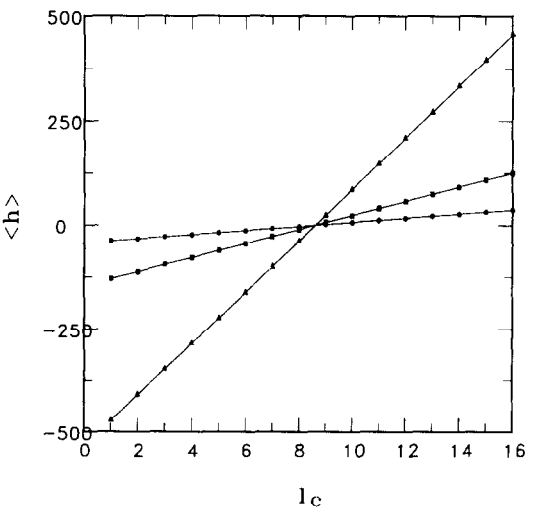

Fig. 5. The average height $\langle h \rangle$ of a sand pile of CLM is plotted with the critical value of the Laplacian l_c for different lattice sizes $L = 10$, 20 and 40 (denoted by circles, squares and triangles, respectively).

In the fig. 6 we see a typical CLM sand pile for $L = 64$. The pile has a very steep rise at the boundaries and in the bulk the pile is almost flat (with a small slope).

We first see how the number of sand grains needed to reach the critical state varies with the system size. Starting from an empty lattice the number of particles n_c needed to add to the system to reach that stage when the average height no longer increases varies with lattice size L as

$$n_c \sim L^4 ,$$

for all values of l_c.

For cluster statistics we simulate two values of l_c, namely $l_c = 8$ and 9. As n_c grows as L^4 we could simulate only small systems $L = 32$, 64 and 128. Though at $l_c = 8$ the average height is negative the system shows the characteristics of a SOC state. We plot the integrated distribution function $D(s)$ with s on the double-logarithmic scale and find that the curves for two values of l_c are almost identical. We present the plot for $l_c = 8$ in fig. 7a. We see that curves for different values of L superpose unless the cluster size sees the finite size of the

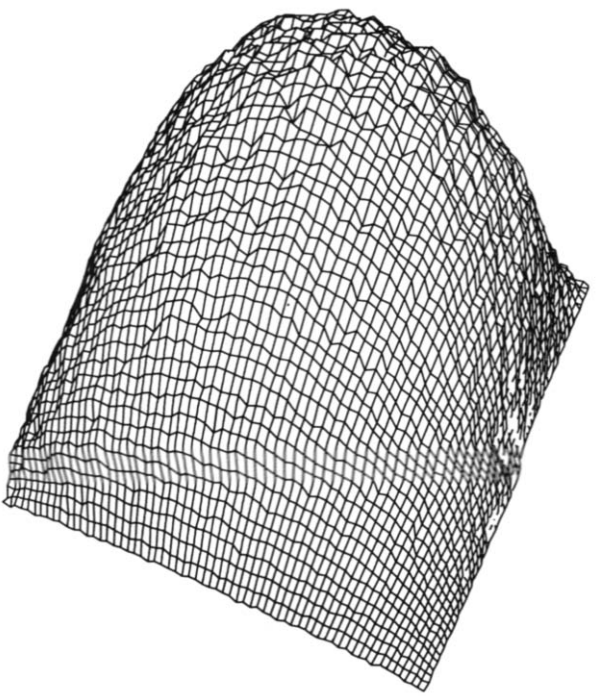

Fig. 6. A typical sand pile in CLM on a square lattice of size $L = 64$ and critical value of the Laplacian $l_c = 9$.

system. The superposed curve has considerable curvature at the beginning but for the lattice size $L = 128$ we get a straight portion over almost two decades. We measure the slope of this region using a least-squares fit and get the value of the exponent to be $\tau = 1.30 \pm 0.03$.

We present the double-logarithmic plot of the integrated life time distribution $D(t)$ with t for $l_c = 8$ in fig. 7b for the same lattice sizes as before.

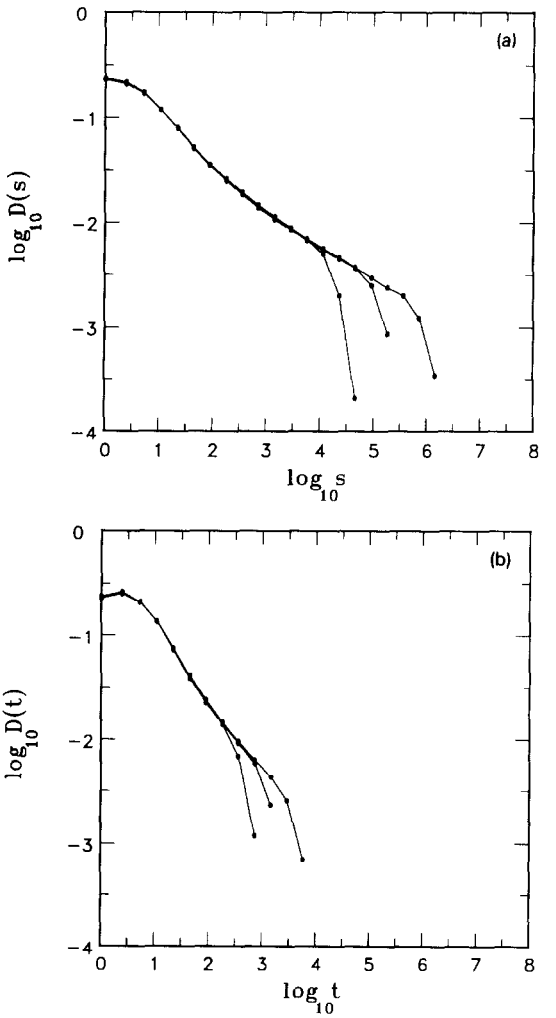

Fig. 7. The cluster statistics for the CLM. (a) The integrated cluster size distribution $D(s)$ is plotted against the cluster size s for lattice sizes $L = 32$, 64 and 128 (from left to the right). (b) The integrated life time distribution $D(t)$ is plotted with the life time t for the same lattice sizes. (c) The average life time T_s for a cluster of size s is plotted against the cluster size s.

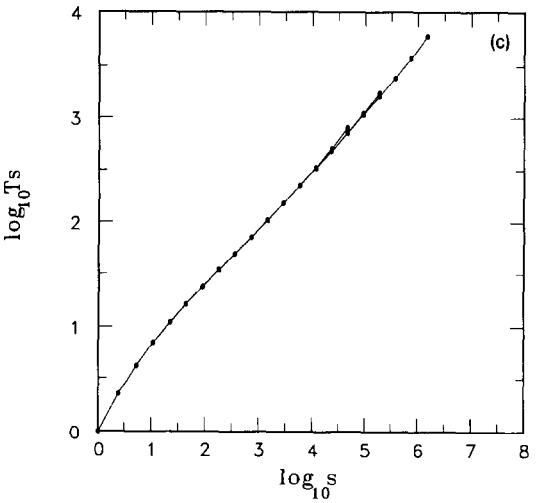

Fig. 7 (cont.).

Here the scaling region is even smaller. We measure the slope of the largest straight portion of the curve for $L = 128$ and obtain a value of $y = 1.57 \pm 0.10$.

Next we calculate how the average life time T_s varies with the cluster size s. For each bin of the cluster size s we calculate the average life time and then plot in a double-logarithmic scale in fig. 7c. We see that the curve is straight apart from the small s values. We measure the slope and get the value of the exponent to be $x = 0.57 \pm 0.05$. We compare this value to the value of $x = 0.53$ obtained using the scaling relation (7).

To get exponents values more accurately we next study a restricted CLM. We now define the following stability condition: if (a) $h_{i,j} \geq 4$ *and* (b) $l_{i,j} \geq l_c$ then the sand column becomes unstable. Condition (a) implies that we do not allow a negative sand column. The height reduction in a toppling and the sand grain additions to the nearest neighbours remain the same as before.

We see first that for $l_c \geq 16$ the condition (a) has no effect in making a toppling because to obtain such an l_c the column must be at least four units in height. Therefore for $l_c \geq 16$ the restricted CLM and unrestricted CLM are the same. On the other hand, for $l_c \leq 4$ the condition (b) has no effect because the minimum value of slope a column of height four units can have is four. Therefore for $l_c \leq 4$ the restricted CLM and CHM with $h_c = 4$ are identical.

To see how the stability condition (a) affects the behaviour when $4 < l_c < 16$ we simulate the restricted CLM for lattice sizes $L = 16$, 32 and 64 for different values of l_c. We consider a large number of steady states (the time interval between two states is large so that they are independent) and calculate the probability of obtaining a steady stage that is not allowed in CHM (with

$h_c = 4$). For a steady state we first check if any site has height greater than or equal to four. If we do not find any we check this configuration if it is an allowed state of CHM (with $h_c = 4$) using the burning algorithm of ref. [13]. In fig. 8 we plot this probability with the value of l_c and see that the probability at a particular value of l_c increases as the system size L increases. In the infinite system size limit the probability appears to jump from zero to one when z_c is changed from four to five. From this study we conclude that in the restricted CLM starting from $l_c = 5$ and onwards all states (for sufficiently large systems) are like CLM and not like CHM (with $h_c = 4$). A transition from the Abelian behaviour to the non-Abelian behaviour would take place when l_c is changed from four to five.

In fig. 9 we plot the average height $\langle h \rangle$ with l_c for two lattice sizes $L = 16$ and 32. We see for $l_c \leq 9$ that the value of $\langle h \rangle$ approaches a fixed value as the lattice size increases $\langle h_L \rangle = \langle h_\infty \rangle - \text{const.}/L$ as in the CHM [9]. The extrapolated average height is slightly greater than the average height in the CHM (with $h_c = 4$). Though all states are non-Abelian, the height is very close to that of CHM (with $h_c = 4$) because the condition for an allowed state of CHM is violated only at a few sites. However, beyond $l_c = 8$, $\langle h \rangle$ increases linearly with l_c for a fixed value of L. The number of particles n_c needed to reach the critical state varies with the lattice size L as $n_c \sim L^2$ for $5 \leq l_c \leq 8$ but $n_c \sim L^4$ for $l_c \geq 9$.

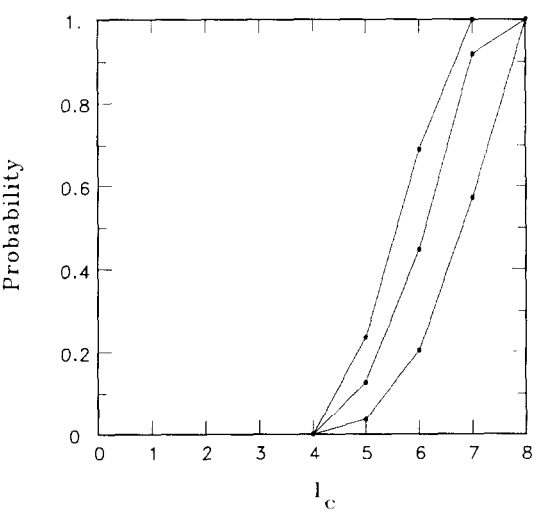

Fig. 8. The probability of getting a restricted CLM steady configuration that is not an allowed configuration in the CHM with $h_c = 4$ is plotted against the critical value of the Laplacian l_c for different lattice sizes $L = 16$, 32 and 64 (from right to the left).

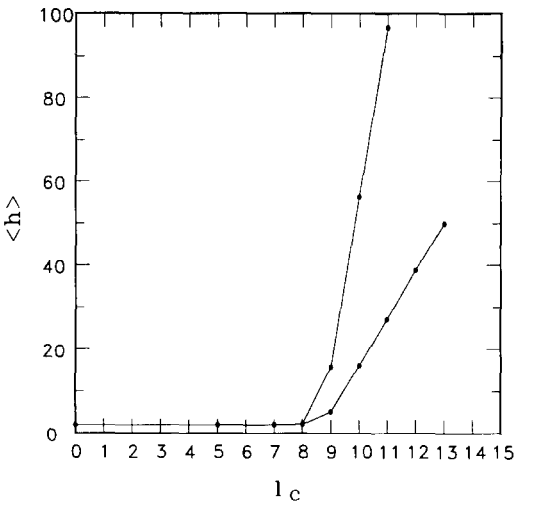

Fig. 9. The average height of the sand pile in the restricted CLM is plotted against the critical value of the Laplacian l_c for different lattice sizes $L = 16$ and 32 (from right to left).

Next we study the avalanche cluster statistics of this restricted CLM for the critical slope $l_c = 8$. For this value of l_c we saw the average heights $\langle h \rangle$ are 2.3607, 2.3696 and 2.3744 for the lattice sizes $L = 256$, 512 and 1024, respectively, approaching the asymptotic limit of 2.379 as $1/L$. We first check that the probability of getting an allowed state of CHM (with $h_c = 4$) is zero for these lattice sizes.

In fig. 10a we plot the integrated distribution $D(s)$ against s on a double-logarithmic scale. We see that the curves have less initial curvature and the scaling region is very prominent and wide compared to the unrestricted CLM curves. All curves almost superpose and we could not find out any systematic variation of the slope. We calculate the slope of the straight portion for the largest lattice. We show the integrated life time distribution $D(t)$ in the fig. 10b and the average life time T_s is plotted in the fig. 10c. In each case we see a much larger scaling region compared to the case of the unrestricted CLM $l_c = 8$, which enabled us to calculate the exponents very accurately. We get $\tau = 1.288 \pm 0.010$, $y = 1.508 \pm 0.030$ and $x = 0.567 \pm 0.003$ for the restricted CLM with $l_c = 8$.

The main advantage of studying the restricted CLM is that for $5 \leq l_c \leq 8$ the critical slowing down is as L^2 instead of the L^4 variation in CLM, which enables us to simulate very large systems. At the same time we see that in the restricted CLM the allowed states of CHM are absent. Therefore we believe that the restricted CLM should be of the same universality class as the ordinary CLM. The small difference in the exponent values result from the small system

size we could simulate for the CLM and for the large curvatures in the distributions. Therefore we conclude that the exponents for the CLM and the restricted CLM are the same and they are $\tau = 1.288$, $y = 1.508$ and $x = 0.567$.

Here we like to mention the two-state model of SOC [15]. In this model in the steady state a site is either empty or occupied by one particle. If more than one particle occupies a certain position at the same time there is a collision and

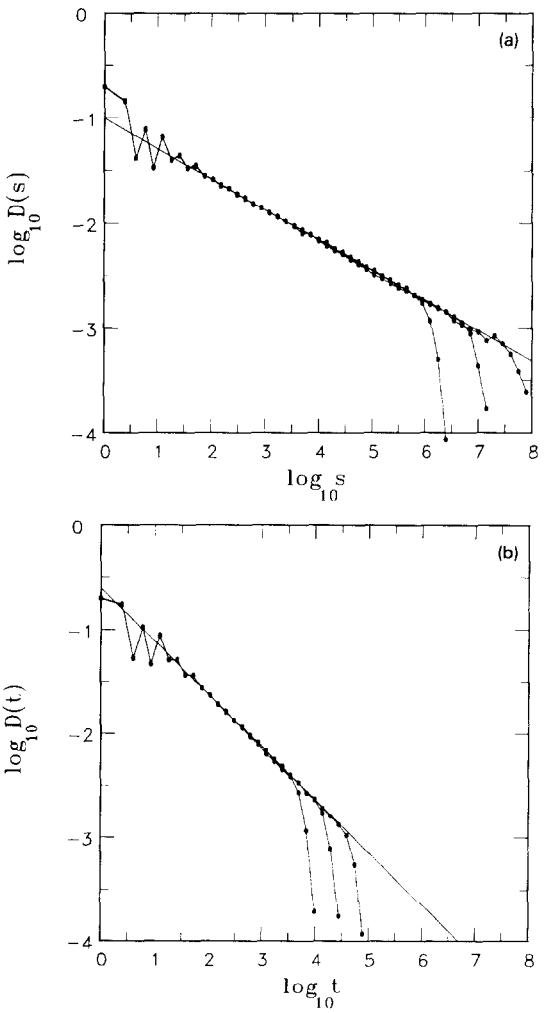

Fig. 10. The cluster statistics for the restricted CLM. (a) The integrated cluster size distribution $D(s)$ is plotted against the cluster size s for lattice sizes $L = 256$, 512 and 1024 (from left to the right). The straight line has a slope of 0.288. (b) The integrated life time distribution $D(t)$ is plotted against the life time t for the same lattice sizes. The straight line has a slope of 0.508. (c) The average life time T_s for a cluster of size s is plotted against the cluster size s. The straight line has a slope of 0.567.

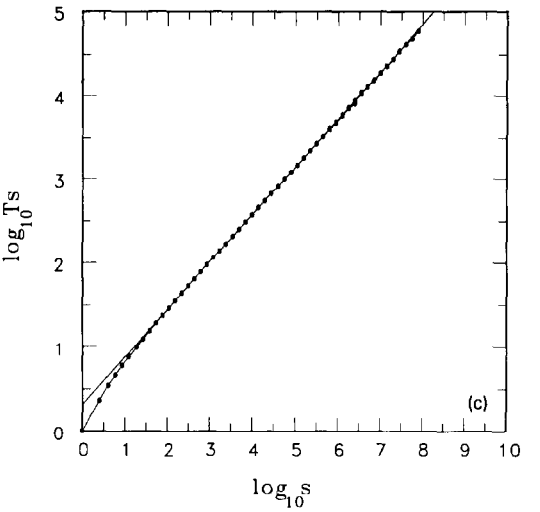

Fig. 10 (cont.).

all the particles randomly jump to the nearest neighbouring sites. We see that all three exponent values of this model are very close to the CLM values. In ref. [15] we thought that this two-state model is a special case of CHM. However, now we believe that as the probability density of a random walker obeys a Laplace equation the two-state model and the CLM belong to the same universality class.

5. Summary

In this paper we have studied three different versions of the sand pile automaton model in two dimensions. These three models are the critical-height (CHM), the critical-slope (CSM) and the critical Laplacian (CLM) models in which the stability of a sand column depends on the zeroth, first and the second derivatives of the local sand height function. Simulating the largest systems and the sample sizes studied so far we could give accurate exponent values for the avalanche cluster distributions in the CHM. We also conjecture for the dominant scaling correction of the avalanche cluster size exponent. In the critical slope model we get sand piles that look somewhat similar to the real sand piles. However, we are unable to see any scaling in the avalanche cluster distribution functions. Finally, in the critical Laplacian model we could get accurate estimates for the exponents defining a restricted CLM. We find that the set of exponents for the CLM are different from that of the CHM and

conclude that the CLM belongs to a different universality class from CHM supporting the conclusion of Kadanoff et al. [10].

We have used around three months of Sun4/Sparc 1 CPU and 7 days of Alliant single processor CPU.

Acknowledgements

I like to thank H.J. Herrmann, J. Kertesz, D. Dhar and H. Puhl for useful discussions and for critical reading of the manuscript.

References

[1] P. Bak, C. Tang and K. Wisenfeld, Phys. Rev. Lett. 59 (1987) 381; Phys. Rev. A 38 (1988) 364.
C. Tang and P. Bak, Phys. Rev. Lett. 60 (1988) 2347.
P. Bak and K. Chen, Physica D 38 (1989) 5.
[2] J. Kertesz and L.B. Kiss, J. Phys. A 23 (1990) L433.
[3] J.H. Jensen, K. Christensen and H.C. Fogedby, Phys. Rev. B 40 (1989) 7425.
[4] H.M. Jaeger, Lie Chu-heng and S.R. Nagel, Phys. Rev. Lett. 62 (1989) 40.
G.A. Held, D.H. Solina, II, D.T. Keane, W.J. Haag, P.M. Horn and G. Grinstein, Phys. Rev. Lett. 65 (1990) 1120.
[5] I.M. Janosi and V.K. Horvath, Phys. Rev. A 40 (1989) 5231.
[6] K.L. Babcock and R.M. Westerfeld, Phys. Rev. Lett. 64 (1990) 2168.
[7] S.S. Manna, L.B. Kiss and J. Kertesz, J. Stat. Phys. 64 (1990) 923.
[8] S.S. Manna, J. Stat. Phys. 59 (1990) 509.
[9] P. Grassberger and S.S. Manna, J. Phys. (Paris) 51 (1990) 1077.
[10] L.P. Kadanoff, S.R. Nagel, L. Wu and S-M. Zhou, Phys. Rev. A 39 (1989) 6524.
[11] Y.-C. Zhang, Phys. Rev. Lett. 63 (1989) 470.
[12] L. Pietronero, P. Tartaglia and Y.-C. Zhang, Physica A 173 (1991) 22.
[13] D. Dhar, Phys. Rev. Lett. 64 (1990) 1613.
S.N. Majumdar and D. Dhar, J. Phys. A 24 (1991) L357.
[14] H. Puhl, HLRZ preprint.
[15] S.S. Manna, J. Phys. A 24 (1991) L363.